Optical properties of light-sensitive liquid-crystal elastomers in the vicinity of the nematic-paranematic phase transition

Marko Gregorc,[1] Hui Li,[2] Valentina Domenici,[3] Gabriela Ambrožič,[4] Martin Čopič,[1,5] and Irena Drevenšek-Olenik[1,5,*]

[1]*Faculty of Mathematics and Physics, University of Ljubljana, Jadranska 19, SI 1001 Ljubljana, Slovenia*

[2]*Nankai University, TEDA APS, 23 Hongda Street, Tianjin 300457, China*

[3]*Dipartimento di Chimica e Chimica Industriale, Università Degli Studi di Pisa, via Risorgimento 35, 56126 Pisa, Italy*

[4]*Center of Excellence for Polymer Materials and Technologies, Tehnološki Park 24, SI 1000 Ljubljana, Slovenia*

[5]*J. Stefan Institute, Jamova 39, SI 1000, Ljubljana, Slovenia*

(Received 6 July 2012; published 20 February 2013)

We investigate light-induced patterning of a monodomain side-chain liquid crystal elastomer (SC-LCE) doped with light-sensitive azobenzene moiety in the temperature region close to the nematic-paranematic phase transition. We show that a strongly nonlinear relationship between the concentration of the *cis* isomers of the azomesogens and the refractive index modification of the material, which is characteristic for the phase transition region, results in nonmonotonous time dependence of the diffraction efficiency of a probe beam. From this effect we determine the sensitivity of the nematic transition temperature on the molar fraction of the *cis* isomers. The relation between the *cis* isomer molar fraction and nematic order also provides a possibility for recording hidden holograms, which can be made visible by cooling the sample from the paranematic to the nematic phase.

DOI: 10.1103/PhysRevE.87.022507 PACS number(s): 61.30.Vx, 42.40.Eq, 61.41.+e

I. INTRODUCTION

Light-sensitive liquid crystal elastomers (LS-LCEs) exhibit very interesting optomechanical properties, which are direct consequences of the specific coupling mechanisms present in these materials [1–3]. When exposed to optical irradiation, they change their size and shape, flip between different shapes, oscillate, or even move on supporting surface [4–11]. Investigations of possible use of these effects in various devices, such as photomechanical transducers, actuators, cantilevers, microfluidic tools, etc., are rapidly expanding [12–18]. Within the increasing enthusiasm for optomechanical response, another very interesting feature of the LS-LCEs, namely, their large opto-optical response, is at present practically overlooked [19,20]. Our recent investigations show that light-induced modifications of optical refractive index in light-sensitive-side-chain LCEs (LS-SC-LCEs) provide a possibility for fabrication of optical diffraction structures (volume holograms), which can be easily tuned by various external stimuli [21].

In the work reported in this paper we focus on light-induced patterning of nematic LS-SC-LCEs in the temperature region close to the nematic-paranematic phase transition, in which several special phenomena, such as an unexpected increase of diffraction efficiency after the writing beams have been turned off, or a possibility of recording "hidden holograms", are observed. By hidden holograms we mean holograms that can be made either visible or invisible, depending on the external parameters, for instance, temperature. Such holograms are very interesting for different watermarking applications, for example, hidden data authentication on medical images, ID cards, product labels, etc. [22,23]. By extending the theoretical model presented in our previous paper to the temperature region in the vicinity of the nematic-paranematic phase transition [24], we show that the observed phenomena can be explained by a nonlinear relationship between molecular modifications induced by the holographic recording process and refractive index of the medium. The nonlinearity is a consequence of the transition from a single-molecular to a cooperative-molecular response.

Nematic LS-SC-LCEs are crosslinked polymer materials composed of four basic constituent units: (i) polymer chains, (ii) crosslinking units, (iii) liquid crystalline (mesogenic) units, and (iv) light-sensitive (photoswitchable) units, such as, for instance, photoisomerizable azobenzene derivatives. Their unique properties originate from strong correlation between the conformational state of the photosensitive molecular units and the conformational state of the polymer chains, which is mediated via a long-range liquid crystalline (LC) ordering of the mesogenic molecular groups [2]. Coupling through the LC order causes a cooperative response, due to which even relatively minor photoinduced perturbations in the concentration of *trans*- and *cis* isomers cause large modifications of the conformation of polymer chains and consequently, of a macroscopic shape of the material. This is the basis of the huge optomechanical response. Besides this, modifications of the LC order and related changes of the material shape also cause large modifications of the optical properties, i.e., optical birefringence of the medium is modified [3,12,25]. This is the origin of the huge opto-optical response that enables efficient recording of volume phase holograms. The recording capability is additionally improved by using so-called monodomain samples [26], which exhibit spatially homogeneous (aligned) orientation of the mesogenic molecular units on a macroscopic scale. Volume holograms based on the same principle can be fabricated also in aligned azo-doped liquid crystalline polymers (LCPs) [27]. However, in LCPs possibilities for their manipulation are considerably restricted due to the need that material stays below the glass transition temperature [20]. In addition to this, in LCPs surface relief gratings are also formed, the properties of which interfere with the properties of the volume holograms [28].

*irena.drevensek@ijs.si

In our experiments a thin film of a LS-SC-LCE was illuminated with UV laser light forming a spatially periodic intensity pattern. Such illumination generates periodic modification of the refractive index of the sample, i.e., it leads to the formation of optical diffraction gratings. The diffractive properties of the gratings were probed by a weak laser beam with wavelength in the visible spectral range. The particularity of our method is that the signal originates solely from the surface region of the sample in which the UV absorption and the associated *trans-cis* isomerization take place [24], whereas conventional investigations probe modifications of the entire volume of the sample. We demonstrate a peculiar behavior of diffraction properties as a function of temperature and time.

II. EXPERIMENTAL RESULTS

Monodomain LS-SC-LCE films with a thickness of 150 μm were prepared according to the two-step "Finkelmann crosslinking procedure" [26]. The polymer backbone is based on a commercial poly(methylhydrosiloxane), which is crosslinked by 1,4-bis(undec-10-en-1-yloxy)benzene used as crosslinker unit. The crosslinker density of the LCE sample used in this work was 5%, as reported in Ref. [29]. As first reported by A. Lebar *et al.* [30] and deeply discussed in a recent review [31], this value of the crosslinking density is low enough to ensure the supercritical behavior at the mesophase transition of nematic side-chain LCEs, limiting the problems of internal fields distribution and sample heterogeneity [32]. The side-chain LC moieties are composed of a standard rodlike mesogen [4-methoxyphenyl 4-(but-3-en-1-yloxy)benzoate] and a light-sensitive azomesogen [(E) -4-(hex-5-en-1-yloxy)-4′-methoxyazobenzene] in the ratio of 9:1. Details of the sample preparation and characterization procedures are described elsewhere [29,33]. In the absence of the UV illumination, the nematic-isotropic (more accurately nematic-paranematic) phase transition occurs at $T_0 = 81.6\,^{\circ}$C, where index 0 denotes zero concentration of the *cis* isomers. The dependence of the associated relative spontaneous elongation of the sample in the direction of the nematic director as a function of temperature is shown in Fig. 1. The solid line is a fit to the model described by Eq. (4).

Optical experiments were performed with films of the size of 3 mm $\times$ 5 mm (see inset of Fig. 1). The upper edge of the film was fixed to the frame on the heating stage, while the lower edge was free to move. However, to prevent bending of the film, the lower edge was loaded with the small weight of a mass of 0.5 g. The resulting stress on the sample is about 10 kPa, which is significantly lower than the typical stress induced by optical irradiation (in case of a clamped sample) [14,33], so we assume that its effects can be neglected. Diffraction gratings were recorded with either two or four intersecting UV laser beams from an argon-ion laser operating at a wavelength of $\lambda_R = 351$ nm. The setup with four beams is described in more detail in [34] and the setup with two beams in [35]. The average power density of UV light on the sample was around 20 mW/cm^2. The lattice distance Λ of the resulting one- and two-dimensional transmission gratings was in the range 1 μm $< \Lambda <$ 15 μm. The polarization of the recording beams was parallel to the nematic director **n**, i.e., the beams were extraordinarily polarized. The diffraction properties of

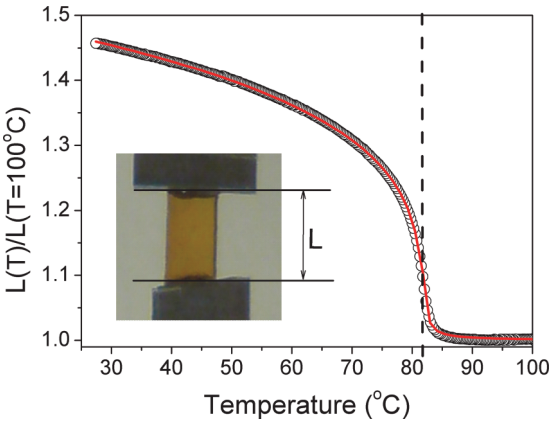

FIG. 1. (Color online) Relative spontaneous elongation of the sample as a function of temperature measured in the absence of UV illumination. Dotted line indicates the transition temperature T_0 accordingly to Eq. (4). Solid line is a fit to Eq. (4). The insert shows a photo of the sample.

the gratings were probed with a low-power beam from a HeNe laser operating at a wavelength of $\lambda_P = 632.8$ nm. The probe beam entered the film at normal incidence and was also extraordinarily polarized. The diameter of the probe beam was about 0.2 mm. The intensities of selected diffraction peaks were detected either with a CCD camera or with photodiodes. The distance between the sample and the detector was 0.5 m. The typical images of far-field diffraction patterns are shown as insets in Figs. 2 and 3. In Fig. 2 one can notice that diffraction peaks are surrounded by elongated scattering patterns, which appear in the direction of the nematic director and are a consequence of the domain structure formed in the sample.

The origin of the recording process is the same at all temperatures, namely, UV illumination-induced *trans*-to-*cis* isomerization of the azomesogene side groups. However, at $T < T_0$ a conformational state of these side groups is strongly

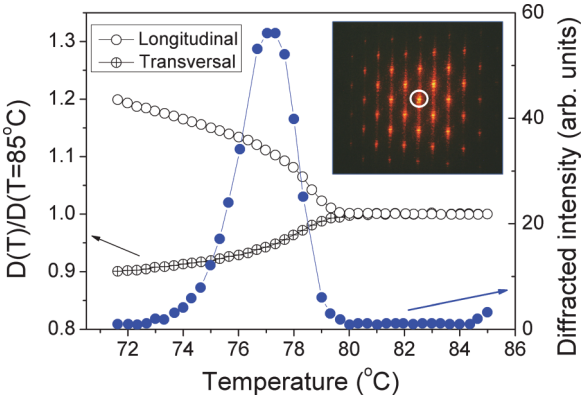

FIG. 2. (Color online) Average intensity of the first order diffraction peaks (solid circles) and relative length of lattice diagonals (open and crossed circles) as a function of temperature during cooling of the sample from $T = 85\,^{\circ}$C to $T = 71\,^{\circ}$C. The inset shows a far-field diffraction pattern at $T = 77\,^{\circ}$C. A white circle designates the transmitted beam. The near neighbor peaks are peaks from the $\{10\}$ family, and the second near neighbor peaks are peaks from the $\{11\}$ family.

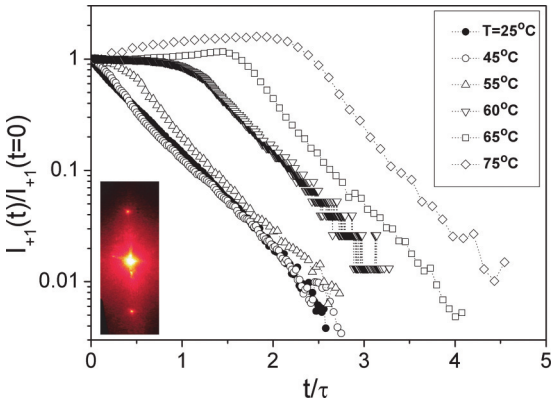

FIG. 3. (Color online) Relative diffraction intensity of the first order diffraction peak as a function of time passed after termination of the recording process at different temperatures. The insert shows the far-field diffraction pattern of the probe beam. The first order diffraction peak is the upper from the three peaks shown in the image. The central peak is the transmitted beam.

coupled with the orientational order of the nonphotosensitive mesogenic side groups, which means that an increased molar concentration of the *cis* groups c_c causes a decrease of the scalar nematic order parameter $S(S = \langle(3\cos^2\theta - 1)/2\rangle$, where θ is the angle between the long axis of the mesogenic molecules and nematic director **n** and the brackets denote averaging). The decrease of S, which is accompanied by the decrease of the ellipticity of the conformation of polymer chains, results in the decrease of the optical birefringence of the material $\Delta n = \Delta(n_e - n_o)$ (where e and o denote extraordinary and ordinary ray, respectively). These modification can be as large as $\Delta n \sim 0.3$ [12,25]. For $T > T_0$, the nematic orientational order is drastically reduced and its coupling with the conformational state of the azomesogenic side groups practically vanishes. Thus modifications of the refractive index take place only via modification of the optical polarizability of azo molecules, i.e., via modification of the single-molecular contribution of the azo molecules to the net refractive index of the material. This response is more than 3 orders of magnitude lower than the cooperative response present at $T < T_0$, so it gives very low diffraction efficiency. One of the possibilities for recording hidden holograms is based on a huge difference of refractive index modifications at $T > T_0$ and $T < T_0$. A holographic pattern that can be recorded either at $T > T_0$ or $T < T_0$ becomes "invisible" by heating the material to $T > T_0$ and can be made visible by cooling the material to $T < T_0$.

Figure 2 shows a result demonstrating a hidden square optical lattice with lattice distance of 13.2 μm. The recording took place at $T = 85\,^{\circ}$C via 3 min of exposure to the UV intensity pattern. Then the sample was cooled to $T = 71\,^{\circ}$C by a cooling rate of $2\,^{\circ}$C/min. Solid circles represent an average diffraction intensity of the first order diffraction peaks (see inset of Fig. 2), i.e., diffraction peaks from the family of Mueller indices $\{10\}$ [34]. In the beginning of the cooling process (at $T = 85\,^{\circ}$C) diffracted intensity is very low and rapidly decreases to the background level. The initial diffraction is a consequence of the thermally induced grating structure, which vanishes within about 1 min. The diffraction intensity then remains at zero down to $T = 80\,^{\circ}$C. Upon further cooling it rapidly increases, reaches a pronounced maximum at $T = 77\,^{\circ}$C, and then decreases. This decrease is a consequence of the two phenomena: (i) cooling below the temperature of the maximum refractive index modulation and (ii) *cis* to *trans* back-isomerization of the azomesogens. Azomesogens used in our material are relatively short lived, i.e., their lifetime in the vicinity of T_0 is about 5 min [35]. This value is very similar to the lifetime of *cis* isomers observed at similar temperatures also in other kinds of LS-SC-LCEs [33].

In addition to the modifications of the diffraction intensity, Fig. 2 also shows modifications of the lattice parameters of the square optical lattice. During transition from the paranematic to the nematic phase, quadratic optical lattice is transformed to the rhombohedral lattice. A relative modification of the diagonal length of the unit cell in directions parallel (longitudinal) and perpendicular (transversal) to the nematic director **n** are calculated from the position of the second order diffraction peaks (diffraction peaks from family $\{11\}$). Our result demonstrates that holographic patterning can be used to investigate details of the shape modifications of the LS-SC-LCEs on the micrometer scale.

Another unusual property that arises in the vicinity of T_0 is an increase of the diffraction efficiency after termination of the recording process, which is in literature known as the hologram dark-enhancement process [36]. As mentioned before, the basis of the holographic recording in LS-SC-LCEs is UV-light-induced *trans* to *cis* isomerization of the azomesogens. Because *cis* isomers have a finite lifetime, their population starts to decrease immediately after the recording. The molar concentration of *cis* isomers $c_c(t)$ exhibits exponential relaxation with lifetime following the Arrhenius activation law and a similar behavior is expected also for the diffraction efficiency. However, this is not always the case. Figure 3 shows the time dependence of a relative intensity of the first order diffraction peak $I_{+1}(t)/I_{+1}(t = 0)$ for a one-dimensional grating structure with $\Lambda = 2.3$ μm at different temperatures. The time scale is given relatively with respect to the spontaneous lifetime of the *cis* state τ at selected temperatures [35]. For temperatures below $50\,^{\circ}$C diffraction intensity decreases exponentially with time, but at $T = 55\,^{\circ}$C, a deviation from exponential relaxation becomes evident, and for $T > 65\,^{\circ}$C, nonmonotonic behavior is observed. At $T = 75^{\circ}$C diffraction intensity measured 4 min after the termination of the recording process is 2 times larger than diffraction intensity measured immediately after the recording. As we show in the theoretical section, this effect can be explained by a nonlinear relationship between c_c and S, which is most pronounced in the vicinity of T_0. Despite the fact that the dark-enhancement effect of diffraction efficiency in our material is much lower than the thermal-enhancement effect shown in Fig. 1, it also provides an option for recording of hidden holograms. This option is particularly interesting, because *cis* to *trans* back-relaxation can be stimulated by optical illumination at a suitable wavelength; therefore the visibility of the recorded patterns can be controlled by optical means.

III. THEORETICAL MODEL AND DISCUSSION

In order to compute the diffraction efficiency as a function of temperature or time after the recording process, we use the

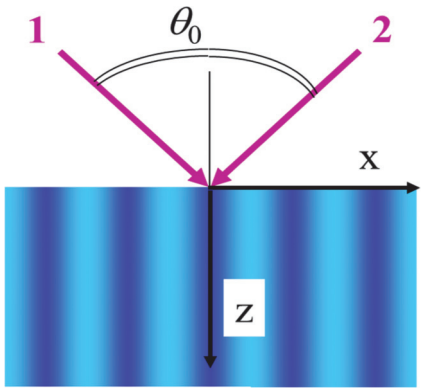

FIG. 4. (Color online) Experimental geometry used for recording of one-dimensional grating structures.

approach presented in our recent paper [24]. Only the case of two-beam interference is considered. However, the approach can be easily extended to four-beam and other multiple-beam interference situations.

The spatial dependence of the molar concentration of the *cis* isomer $c_c(\mathbf{r},t)$ is determined by the absorption of the two UV laser beams crossed in the sample. As the modification in the isomer distribution is slow compared to the propagation time of light through the sample, we can model the recording process by first calculating the light field $E(\mathbf{r},t)$ in the sample at a certain spatial dependence $c_c(\mathbf{r},t)$, and then calculate the corresponding local change $\Delta c_c(\mathbf{r},t)$. The effect of $\Delta c_c(\mathbf{r},t)$ on the local absorption coefficient is then taken into account in the calculation of the light field $E(\mathbf{r},t+\Delta t)$.

We consider two laser beams crossing in the LCE film at an angle θ_0. Let x be the axis in the plane of the film and z the surface normal (Fig. 4). Optical electric field E with angular frequency ω_R is assumed to be parallel to the y axis. Propagation of light in the sample with some inhomogeneous distribution of the *trans* and *cis* isomers can best be described by using the paraxial wave equation. For this we first write the electric field in the form $E = (\mu_0/\varepsilon_0)^{1/4}(2\hbar\omega_R/\bar{\varepsilon})^{1/2}\psi(x,z)\exp(ikz)$ with $k = \sqrt{\bar{\varepsilon}k_0^2 - (q/2)^2}$, where $\bar{\varepsilon}$ is the real part of the average optical dielectric constant of the medium, k_0 is the magnitude of the wave vector in vacuum, and $q/2 = k_0\sin(\theta_0/2)$ is the transverse component of the incident wave vector of each beam. The amplitude function ψ is normalized so that its square gives the photon flux density. It is assumed to be a slow function of z, so that it satisfies the paraxial wave equation

$$-2ik\frac{\partial\psi}{\partial z} = \frac{\partial^2\psi}{\partial x^2} - i\varepsilon''(x,z)k_0^2\psi. \tag{1}$$

The term associated with the modulated part of the real dielectric function is omitted in Eq. (1), as at the recording wavelength λ_R its contribution is much smaller than the contribution of the imaginary part. The imaginary part of the dielectric function ε'' depends on the molar concentration of the *trans* and *cis* isomers. It can be expressed as

$$\varepsilon'' = [\sigma_t c_t(x,z) + \sigma_c c_c(x,z)]/k_0, \tag{2}$$

where σ_t and σ_c are the absorption cross sections (in units of m^2) of the *trans* and *cis* isomers, and $c_t(x,z)$ and $c_c(x,z)$ are the respective molar concentrations of the *trans* and *cis* azomesogens (in units of moles/m^3). The absorption band of azobenzene derivatives in *trans* conformation has a peak at $\lambda_t \sim 350$ nm, while the *cis* isomers absorb mainly in the visible region, but there is some overlap of the absorption bands at the recording laser wavelength λ_R.

The concentrations c_t and c_c at any point in the sample are given by the equations

$$\frac{dc_t}{dt} = [-\eta_t\sigma_t c_t + \eta_c\sigma_c c_c]|\psi|^2 + \frac{c_t}{\tau} \quad \text{and } (c_c + c_t) = c_A, \tag{3}$$

where η_t and η_c are constants describing the conversion efficiency from the electronic excited state to the *cis* or *trans* conformation, τ is the thermal lifetime of the *cis* state, and c_A is molar concentration of the azomesogens. For our material $c_A \sim 500$ mol/m^3 [29]. The value of c_A is proportional to the relative molar fraction of azomezogenes with respect to all mezogenes $\chi_A = N_A/(N_A + N_S)$, where N_A and N_S denote number of azomesogens and standard (nonphotosensitive) mesogens, respectively. In our material the value of χ_A was 0.1.

To simultaneously take into account the effects of absorption and diffraction of the writing beams on the periodic distribution of the two isomers, we numerically solve the paraxial wave equation with the initial condition given by the interference of the two writing beams. The amplitudes of the two beams need not be exactly equal, so the initial condition at the input surface of the sample (at $z = 0$ and $t = 0$) is $E = E_1 e^{iqx/2} + E_2 e^{-iqx/2}$.

Both the paraxial wave equation [Eq. (1)] and the rate equations [Eq. (3)] are solved numerically on a suitably chosen mesh. Usually we use 40 × 100 mesh points. The number of time steps depends on the assumed recording time and goes up to around 1000. Further details on the calculation are given elsewhere [24].

The diffraction efficiency for the first order diffraction peaks in the vicinity of Bragg angle depends on the first Fourier component of the spatial modulation of optical dielectric function $\varepsilon(\mathbf{r})$ with respect to the transverse wave number q. $\varepsilon(\mathbf{r})$ is periodically modulated in the direction of x due to the change in the order parameter S that is caused by the change in c_c. In our previous paper we assumed that modification of the dielectric function associated with extraordinary polarized optical radiation $\delta\varepsilon = \varepsilon(c_c) - \varepsilon(c_c = 0)$ is proportional to c_c [24]. This assumption is suitable at temperatures far below the phase transition from the nematic to the paranematic phase (T_0) but it fails close to T_0. However, in nematic phase $\delta\varepsilon$ is proportional to δS, so in order to obtain $\delta\varepsilon$ from the calculated spatial profile of c_c we need to establish a proper connection between S and c_c.

We first need a functional form describing $S(T)$. This is proportional to $(l-1)$, where $l = L(T)/L(T \gg T_0)$ is the spontaneous relative elongation of the sample on cooling from the isotropic phase, shown in Fig. 1. To fit the data in Fig. 1 we constructed a heuristic function:

$$l(T) - 1 = Af(T,T_0) = A\{[(1 + B|T - T_0|^\alpha)/B]^{1/\alpha} - (T - T_0)\}^{1/(\alpha-1)}. \tag{4}$$

This function has the property that for $T < T_0$ it behaves like $A\,(T_0 - T)^{1/(\alpha-1)}$ and for $T > T_0$ as $[C\,(T - T_0)]^{-1}$ with $C = (\alpha B)^{1/(\alpha-1)}$, as expected for the first order phase transition in a field that is above the critical value. As is evident from Fig. 1, this function fits the experimental data very well with $T_0 = 81.6\,^{\circ}$C, $\alpha = 4.8$, and $B = 29$. The supercritical nature of the transition in our sample is due to the internal strain field, which is caused by the two-step crosslinking procedure.

It is worth noting that the above-given fitting function describes surprisingly well theoretical dependence of the order parameter on temperature in a wide interval for Landau-type free energies with third, fourth, and sixth order terms in order parameter, and an applied conjugate field that is large enough to make the transition supercritical. Different relative magnitudes of the Landau coefficients only change the value of the parameter α that ranges from 3 for a second order transition with only the fourth order term to between 5 and 6 for a discontinuous transition with a large positive sixth order term.

After obtaining the functional form of $S(T) \propto (l - 1)$ in our LS-SC-LCE material, we can further address the problem of dielectric function modulation $\delta\varepsilon$ as a function of molar concentration of *cis* azomesogens c_c. The *cis* azomesogens act as impurities in the nematic phase. It is well known that the effect of impurities on the nematic-isotropic transition is to shift the transition temperature to lower values. We assume that the shift is proportional to molar fraction of *cis* azomesogens with respect to all mesogens $\chi_{Ac} = N_{Ac}/(N_A + N_S)$, i.e., that $T_0(\chi_{Ac}) = T_0 - a_\chi \chi_{Ac}$, where $N_{Ac} = N_A - N_{At}$ denotes number of azomesogens in the *cis* state, N_{At} denotes number of azomesogens in the *trans* state, and a_χ governs the "sensitivity" of the transition temperature T_0 to the presence of the *cis* "impurities" [2,4]. Taking into account the volume conservation of the LCE material [1], it follows that $\Delta c_c(T) \propto \Delta\chi_{Ac}(T)$, from which it follows that spatial modulation of a component of the optical dielectric tensor ε_i associated with an extraordinarily polarized optical beam can be described as

$$\delta\varepsilon_i(T,c_c) = \varepsilon_i(T,c_c) - \varepsilon_i(T \gg T_0) = Cf(T,T_0 - ac_c), \quad (5)$$

where C is a scaling constant that could be obtained by measuring the indices of refraction (birefringence) at a given temperature T and a is a constant that is proportional to a_χ, namely, for our material $(a/a_\chi) \sim (2 \times 10^{-4}\ \mathrm{m}^3/\mathrm{mol})$. Due to high absorption and optical imperfections, the measurements of birefringence for UV light in our samples is not possible. Much thinner samples would be needed. However, the value of C affects only the absolute value of the diffraction efficiency of the recorded grating, but does not influence the functional form of the dependence of diffracted intensity on T or time delay after recording.

Some examples of the calculated spatial profiles of $\chi_{Ac}(x,z)$ and $\delta\varepsilon_i(x,z)$ are shown in Fig. 5. The values of the absorption cross sections of the *cis*- and *trans*-isomers and for the conversion efficiency to the *cis* conformation were taken from Ref. [24]. The profile of $\chi_{Ac}(x,z)$ is virtually the same at all temperatures, while the profile of $\delta\varepsilon_i(x,z)$ strongly depends on the temperature. At low temperatures [Fig. 5(b)] the amplitude of the modulation of $\delta\varepsilon_i$ is small due to weak dependence of the order parameter on temperature, while very close to T_0 it is small due to the low value of the order parameter [Fig. 5(d)].

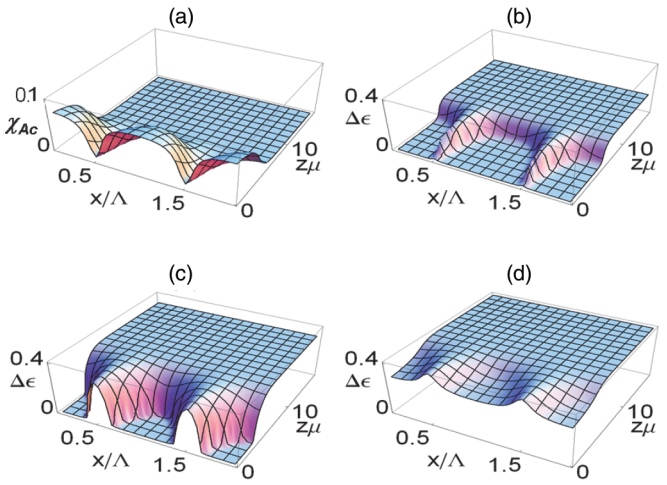

FIG. 5. (Color online) (a) Spatial distribution of molar fraction of *cis* azomesogens with respect to all mesogens $\chi_{Ac}(x,z)$ after 5 min of exposure to UV interference pattern. The associated spatial distribution of $\delta\varepsilon_i(x,z)$: (b) at $T = 30\,^{\circ}$C, (c) at $T = 55\,^{\circ}$C, and (d) at $T = 80\,^{\circ}$C.

The maximum modulation amplitude is achieved at around $T = 55\,^{\circ}$C. Besides the modulation amplitude, the intensity of the first order diffraction peaks also depends on the shape of the modulation, as sharper peaks along the x axis give a lower value of the first Fourier coefficient at the transverse wave vector q.

In Fig. 6 we show the calculated value of the square of the z-averaged first Fourier component of $\delta\varepsilon_i(x,z)$, which is proportional to the diffraction efficiency of the first order diffraction peaks $\eta_{\pm1} = I_{\pm1}/I_0$, where I_0 is incident intensity of the probe beam, as a function of temperature for a grating that was recorded in the paranematic phase. At $T > T_0$ there is practically no diffraction. The sudden increase of the calculated value of $\eta_{\pm1}$ below T_0 is very similar to the abrupt increase of the diffracted intensity observed in the experiment (Fig. 2). Since the cooling rate in the experiment was on the same time scale as the rate of the *cis* to *trans* back-relaxation, the spontaneous decay of the grating during the cooling process was also included in the computation. With

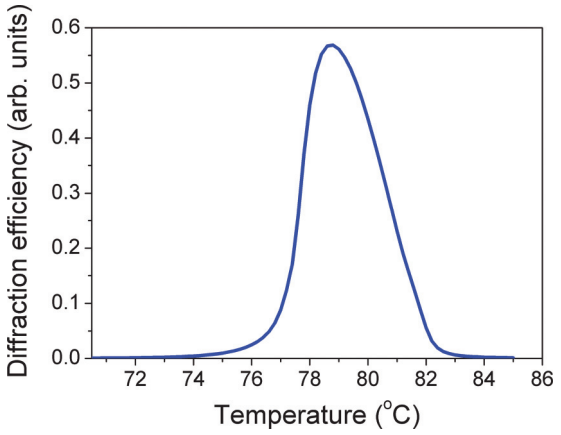

FIG. 6. (Color online) Calculated diffraction efficiency during cooling from $T = 85\,^{\circ}$C to $T = 71\,^{\circ}$C.

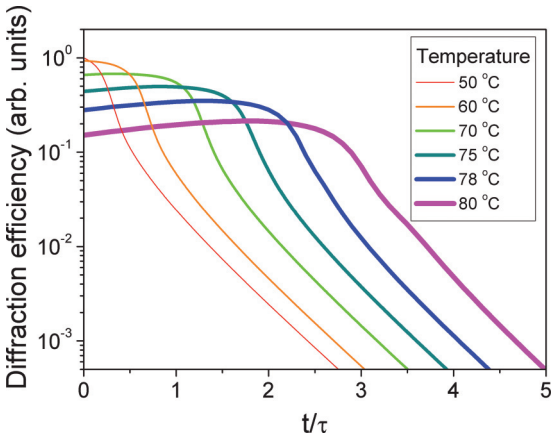

FIG. 7. (Color online) Calculated diffraction efficiency during spontaneous relaxation of the grating at different temperatures.

this addition a very good agreement between the computational and the experimental result is obtained.

In Fig. 7 we show the calculated dependence of $\eta_{\pm 1}$ on the elapsed time after recording the grating at fixed temperature T. One can notice that when T is close to T_0 the value of $\eta_{\pm 1}$ first increases and only later it starts to exponentially decrease. By comparing these curves with the experimental results (Fig. 3) we deduced the value of the sensitivity parameter a_χ. This was performed so that the value of a_χ used in the simulations was adjusted so that the calculated curves $\eta_{\pm 1}(t)$ started to exhibit a nonmonotonic dependence at $T = 55 \pm 5\,^\circ$C, as was observed in the experiments. The corresponding value of a_χ is 600 ± 60 K. Therefore, if all azomesogens in our material were excited to the *cis* state, the nematic-paranematic phase transition would decrease to room temperature. This result seems to be reasonable. Very approximately, one can expect that at maximal molar fraction of *cis* azomesogens with respect to all mesogens, which is $\chi_{Ac,\,\max} = \chi_A = N_A/(N_A + N_S) = 0.1$, the nematic order is "diluted" by 10%, so that the expected change of the critical temperature $\Delta T_0/T_0$ is $0.1 \times T_0$, which is 35 K. The large value of a_χ is a basis for efficient holographic recording.

The value of parameter a_χ is also of fundamental importance for different possible applications of the LS-SC-LCEs, especially since at present shape changes of LCEs driven by light seem to be the most promising method for applications. With our method a_χ can be determined also for thick samples in which light-induced modifications take place only in a surface layer of the sample. Investigations of conventional thermotropic liquid crystals doped with 10% of an azobenzene derivative revealed a downshift of the nematic-isotropic transition temperature in the range of tens of K [37], which is in agreement with our findings.

Previous measurements in LCE reported a much smaller reduction of the transition temperature at similar concentrations of the azobenzene moieties [4]. In those experiments the change was measured by monitoring sample deformation after long-time exposure to UV radiation. Due to the thermally and light-driven transitions back to the *trans* state, there is a considerable stationary absorption of the UV light, causing only a part of the thickness of the sample to be transformed. The measured distortion of the sample is therefore smaller than it would be if all the azobenzene would be converted to the *cis* isomer.

IV. CONCLUSIONS

Our experiments show that a periodic distribution of the *cis* isomer that produces nearly undetectable optical diffraction in the paranematic phase of the LS-SC-LCE becomes readily observable when the sample is cooled to the nematic phase. In the material used in our study the lifetime of the *cis* isomer at elevated temperatures is relatively short, of the order of minutes, so hidden diffraction patterns can be observed only for short time. But by incorporating photosensitive moieties with much slower *cis* to *trans* back-relaxation, such as, for instance, thermally irreversible fulgides [38], the lifetimes of recorded holographic structures can be made much longer.

Besides temperature-induced modifications, another very intriguing possibility to make holograms visible or invisible is by stretching the LCE film. This could be achieved if illumination with patterned UV light took place at the second crosslinking stage of the two-step fabrication process [25,39]. The UV intensity would modulate the strength of the internal orienting elastic field, which governs the threshold of the semisoft response on stretching in the direction perpendicular to the nematic director [40]. In this situation the director starts to rotate at a particular threshold value of the strain. If the threshold is spatially inhomogeneous, strain slightly above the threshold would produce a visible hologram that would otherwise be unobservable.

In addition to demonstration of peculiar holographic features of the LS-SC-LCEs in the vicinity of the nematic-paranematic phase transition, our experiments also enable us to obtain the sensitivity of the nematic transition temperature on the concentration of the *cis* isomers, an important parameter related to photoinduced response of the LS-SC-LCE materials.

ACKNOWLEDGMENTS

We acknowledge financial support from the Ministry of Higher Education, Science and Technology of the Republic of Slovenia through Contract No. 3211-10-000057 (Centre of Excellence for Polymer Materials and Technologies) for financing the research on synthesis of LS-LCEs; Research Program P1-0192, Light and Matter for Financing Research on Optical Properties; and Bilateral Project BI-CN/11-13-012 for supporting the visit of H. Li to Ljubljana.

[1] M. Warner and E. M. Terentjev, *Liquid Crystal Elastomers* (Oxford University Press, New York, 2007).

[2] H. Finkelmann, E. Nishikawa, G. G. Pereira, and M. Warner, Phys. Rev. Lett. **87**, 015501 (2001).

[3] D. Corbett and M. Warner, Liq. Cryst. **36**, 1263 (2009).

[4] P. M. Hogan, A. R. Tajbakhsh, and E. M. Terentjev, Phys. Rev E **65**, 041720 (2002).

[5] Y. L. Yu, M. Nakano, and T. Ikeda, Nature (London) **425**, 145 (2003).
[6] M. Warner and L. Mahadevan, Phys. Rev. Lett. **92**, 134302 (2004).
[7] N. J. Dawson, M. G. Kuzyk, J. Neal, P. Luchette, and P. Palffy-Muhoray, J. Opt. Soc. Am. B **28**, 1916 (2011).
[8] H. Y. Jiang, S. Kelch, and A. Lendlein, Adv. Mater. **18**, 1471 (2006).
[9] U. Hrozhyk, S. Serak, N. Tabiryan, T. J. White, and T. J. Bunning, Opt. Express **17**, 716 (2009).
[10] K. M. Lee, M. L. Smith, H. Koerner, N. Tabiryan, R. A. Vaia, T. J. Bunning, and T. J. White, Adv. Funct. Mater. **21**, 2913 (2011).
[11] M. Camacho-Lopez, H. Finkelmann, P. Palffy-Muhoray, and M. Shelley, Nature Mater. **3**, 307 (2004).
[12] J. Cviklinski, A. R. Tajbakhsh, and E. M. Terentjev, Eur. Phys. J. E **9**, 427 (2002).
[13] C. L. M. Harvey and E. M. Terentjev, Eur. Phys. J. E **23**, 185 (2007).
[14] A. Sanchez-Ferrer, Proc. SPIE **8107**, 810702 (2011).
[15] M. H. Li, P. Keller, B. Li, X. Wang, and M. Brunet, Adv. Mater. **15**, 569 (2003).
[16] C. L. van Osten, C. W. M. Bastiaansen, and D. J. Broer, Nature Mater. **8**, 677 (2009).
[17] S. V. Serak, N. V. Tabiryan, T. J. White, and T. J. Bunning, Opt. Express **17**, 15736 (2009).
[18] M. H. Li and P. Keller, Philos. Trans. R. Soc. A **364**, 2763 (2006).
[19] E. Sungur, M. H. Li, G. Taupier, A. Boeglin, M. Romeo, S. Mery, P. Keller, and K. D. Dorkenoo, Opt. Express **15**, 6784 (2007).
[20] Y. Zhao, in *Smart Light Responsive Materials*, *Azobenzene-Containing Polymers and Liquid Crystals*, edited by Y. Zhao and T. Ikeda (John Wiley & Sons, Hoboken, NJ, 2009), p. 363.
[21] M. Devetak, B. Zupancič, A. Lebar, P. Umek, B. Zalar, V. Domenici, G. Ambrožič, M. Žigon, M. Čopič, and I. Drevenšek-Olenik, Phys. Rev. E **80**, 050701 (2009).
[22] R. A. Lee and P. W. Leech, Microelectron. Eng. **83**, 2004 (2006).
[23] D. Kundur and D. Hatzinakos, IEEE Trans. Multimedia **6**, 185 (2004).
[24] M. Gregorc, B. Zalar, V. Domenici, G. Ambrožič, I. Drevenšek-Olenik, M. Fally, and M. Čopič, Phys. Rev. E **84**, 031707 (2011).
[25] Y. Yusuf, N. Minami, S. Yamaguchi, D. U. Cho, P. E. Cladis, H. R. Brand, H. Finkelmann, and S. Kai, J. Phys. Soc. Jpn. **76**, 073602 (2007).
[26] J. Kupfer and H. Finkelmann, Makromol. Chem., Rapid Commun. **12**, 717 (1991).
[27] M. Eich and J. Wendorff, J. Opt. Soc. Am. B **7**, 1428 (1990).
[28] A. Natansohn and P. Rochon, Chem. Rev. **102**, 4139 (2002),
[29] V. Domenici, G. Ambrožič, M. Čopič, A. Lebar, I. Drevenšek-Olenik, P. Umek, B. Zalar, B. Zupančič, and M. Žigon, Polymer **50**, 4837 (2009).
[30] A. Lebar, Z. Kutnjak, S. Zumer, H. Finkelmann, A. Sanchez-Ferrer, and B. Zalar, Phys. Rev. Lett. **94**, 197801 (2005).
[31] V. Domenici, Prog. Nucl. Magn. Reson. Spectrosc. **63**, 1 (2012).
[32] W. H. de Jeu, E. P. Obraztsov, B. I. Ostrovskii, W. Ren, P. J. McMullan, A. C. Griffin, A. Sanchez-Ferrer, and H. Finkelmann, Eur. Phys. J. E **24**, 399 (2007).
[33] A. Sanchez-Ferrer, A. Merekalov, and H. Finkelmann, Macromol. Rapid Commun. **32**, 672 (2011).
[34] M. Devetak, J. Milavec, R. A. Rupp, B. Yao, and I. Drevenšek-Olenik, J. Opt. A: Pure Appl. Opt. **11**, 024020 (2009).
[35] M. Gregorc, H. Li, V. Domenici, G. Ambrožič, M. Čopič, and I. Drevenšek-Olenik, Materials **5**, 741 (2012).
[36] H. Liu, D. Yu, X. Li, S. Luo, Y. Jiang, and X. Sun, Opt. Express **18**, 6447 (2010).
[37] G. G. Nair, K. Prasad, and C. V. Yelamaggad, J. Appl. Phys. **87**, 2084 (2000).
[38] Y. Yokoyama, Chem. Rev. **100**, 1717 (2000).
[39] C. H. Legge, F. J. Davis, and G. R. Mitchell, J. Phys. II (France) **1**, 1253 (1991).
[40] M. Warner, P. Bladon, and E. M. Terentjev, J. Phys. II (France) **4**, 93 (1994).